Direct Tensile Behavior of a Transversely Isotropic Rock

JYH JONG LIAO†
MING-TZUNG YANG†
HUEI-YANN HSIEH†

The tensile behavior of a transversely isotropic rock is investigated by a series of direct tensile tests on cylindrical argillite specimens. To study the deformability of argillite under tension, two components of an electrically resistant type of strain gage with a parallel arrangement, or a semiconductor strain gage, are adopted for measuring the small transverse strain observed on specimens during testing. The curves of axial stress vs axial strain and vs average volumetric strain are presented for argillite specimens with differently inclined angles of foliation. Experimental results indicate that the stress–strain behavior depends on the foliation inclination of specimens with respect to the loading direction. The five elastic constants of argillite are calculated by measuring two cylindrical specimens in the manner recommended by Wei and Hudson. Based on theoretical analysis results, the range of the foliation inclination of the specimens tested is investigated for feasibility obtaining the five elastic moduli. A dipping angle of the foliations (θ) of 30–60° with respect to the plane normal to the loading direction is recommended. The final failure modes of the specimens are investigated in detail. A sawtoothed failure plane occurs for the specimens with a high inclination of foliation with respect to the plane perpendicular to the loading direction. On the other hand, a smooth plane occurs along the foliation for specimens with low inclination of foliation with respect to the plane normal to the loading direction. A conceptual failure criterion of tensile strength is proposed for specimens with a high inclination of foliation. © 1997 *Elsevier Science Ltd*

INTRODUCTION

It is well-known that rocks are less resistant to tension than to compression or shear. Tension cracks often develop before compression or shear failure. E.g. rock bridges in non-connected joints may fracture by tension before shear failure. Tensile cracks are often observed in the upper surface of a failed slope, in the circumference of a borehole or a tunnel with internal pressure, and in rocks immediately after drilling or blasting [1]. These phenomena provide evidence of direct tensile failure in rock structures. Thus, an understanding of the rock behavior under tension can be beneficial in the analysis that involves either intact rock or rock masses. However, direct measurements of tensile properties of rocks, such as strength and deformability are difficult either in the laboratory, or in the field. It has sometimes been

common practice to neglect tensile properties (or replace tensile properties by compressive properties) as an input parameter in the engineering analysis. The tensile behavior of different rock formations can vary considerably, and neglecting such a parameter may lead to unreliable results. This drawback is further manifested in numerical analyses or simulations that involve rocks under tension. Obviously, the tensile behavior of rock formations must be understood in detail before designing or building such structures in such locations.

Many rocks are anisotropic due either to the processes which form rocks, or to later processes which move and deform them. The mechanical properties and behavior of anisotropic rocks under tension, or compression vary with direction. This variation often relates to the existence of well-defined rock fabric elements in the form of bedding, stratification, layering and foliation. In most practical cases, anisotropic rocks can be modeled either as orthotropic or transversely isotropic materials.

†Dept of Civil Engng, National Chiao-Tung University, 1001 Ta Hsueh Rd, Hsinchu, Taiwan 30050, Republic of China.

Orthotropy implies that three orthogonal planes of elastic symmetry exist at any point in the rock and that these planes have the same orientation throughout. Transverse isotropy implies that, at any point in the rock, there is an axis of symmetry of rotation and that the rock has isotropic properties in a plane normal to this axis. This is called the plane of transverse isotropy [2]. Transverse isotropy is generally characteristic of foliated metamorphic rocks (e.g. argillite, slate, phyllite and gneiss) and stratified sedimentary rocks (e.g. shale and sandstone). Engineering analysis must take account of the mechanical properties and behavior of such rock [3].

Many authors [4–10] have investigated in detail the mechanical properties of transversely isotropic rocks under compression. They conclude that the compressive strength, triaxial shear strength, fracture behavior and deformability of anisotropic rocks vary according to the inclination of the discontinuities in specimens. The failure criteria for the triaxial peak strength of transversely isotropic rocks under compression have been well established from both empirical and theoretical standpoints. Indirect tensile tests, such as the Brazilian test, are commonly used to determine the tensile strength of isotropic rocks. However, they are not appropriate for anisotropic rocks: this is because they are neither exact anisotropic solutions [11–13] for interpreting test results, nor can actual tensile fracture behavior be observed and measured during the testing of anisotropic rocks. Nor can numerical results be directly applied to determine the tensile strength [14] involved. The direct tensile test, therefore, is an appropriate method for determining the mechanical properties and behavior of anisotropic rocks under tension. However, to date, the direct tensile test has rarely been employed in rock mechanics laboratories. This is because both the bending stresses, or torsion moment (caused by the eccentricity of machine axial loads) and the anomalous concentrated stresses (induced by an improper connection during testing between the ends of a rock specimen and the machine caps serving to transfer the tensile loads to the specimen) are frequently unavoidable [15, 16]. The efficient performance of a pure tensile test requires a verified tensile grip, associated with a testing machine of high quality. For this study, a reliable testing machine with servocontrolled functions and a pair of verified tensile grips were adopted.

In the past, different investigators have designed various types of tensile grips for direct tensile tests [15–19]. Typically, a tensile grip comprises two parts: a specimen-connecting part and a load-transferring part. Barla and Goffi [15] used the finite element method to evaluate how the connection methods to the load-transferring mechanism affect the induced stress distribution in the specimen. The load-transferring mechanisms evaluated in their computations included cementation of the specimen to a metal cap by epoxy-resin and the use of a mechanical grip. The conclusion according to Barla and Goffi was that the former connection method creates a more uniform stress distribution within the specimen than the latter. A mechanical holder was convenient for sample assembly. However, the evidence of failed specimens indicated that, when this type of grip was employed, the stress concentration was usually induced at the ends of specimens [16, 17].

In this investigation, the cement method is recommended for direct tensile tests. Two types of load transmitter were used to transfer the tensile loads from the testing machine to the specimen and to overcome the bending stress, or torsion moment in the specimen. One was a flexible type, such as a roller or a link chain [18, 19] and the other was a stiff type, such as an elastic joint [15] or a steel rod with ball joints [16, 17]. The flexible type was suggested for transferring the axial load, because it effectively reduced the bending in the specimen. However, if the flexible type is employed, a torsion moment induced in the specimen may occur and the unpredictable motion of the flexible chain if the specimen fails may damage the testing machine, or endanger users. Adopting a stiff type of load transmitter may easily induce bending stress in the specimen. Nevertheless, we believe that this can be overcome by employing a well designed and manufactured stiff rod, and an associated part for eliminating the eccentricity of the axial load of the testing machine, such as a ball joint of high quality provides.

For studying the mechanical behavior of rocks, in addition to the induced stresses, tests for measuring induced displacement must be included. Certain investigators [15, 16] have tried to measure the axial strain and transverse strain in specimens of transversely isotropic rocks by an electrically resistant type of linear strain gage under direct tensile testing. Due to the small transverse strain with the same order of magnitude as the instrument precision, only the axial strains recorded were reliable. Neither the five true elastic moduli nor the complete stress–strain relation of transversely isotropic rocks have been presented in the previous literature. Several authors [12, 13, 16] have proposed some theoretical or phenomenological failure criteria for the tensile strength of anisotropic rocks to match the testing data. Most of these failure criteria exhibit considerable error compared with the experimental results obtained from specimens with a high inclination of elastic symmetry planes corresponding to the cross section of cylindrical specimens.

This study investigates the tensile behavior of transversely isotropic rocks under tension by conducting a series of direct tensile tests on argillite. A material testing machine associated with verified tensile grips is employed for the tests. To monitor the very small strain on rock specimens, semiconductor strain gages and electrically resistant strain gages with special arrangements are adopted. The five elastic moduli of argillite under tension are calculated from the measured strains of a pair of rock specimens with different inclinations of foliation. Relations of uniaxial stress–uniaxial strain–volumetric strain in uniaxial tensile tests are also

presented. No similar results have been thought to have been reported previously. Finally, a failure criterion based on a conceptual failure mode of argillites in pure tension is proposed.

TESTING EQUIPMENT, SAMPLE PREPARATION AND ROCK DESCRIPTION

A servocontrolled material testing machine (model MTS 810) with the tensile grip described below was employed for direct tensile tests. MTS 810 is a computer controlled machine with 250 kN load capacity. The software Testlink was utilized to conduct computer controlled tests. A test can be performed with stress control (in tension or in compression) or with strain control (in tension or in compression). Load (measured by a 250 kN load cell), displacement (measured by a LVDT) and strain (measured by an extensometer) may serve as the control parameter. To satisfy the two main considerations regarding the design of a grip, a stiff rod type with three pairs of ball joints was devised for this study (Fig. 1). It is similar to the apparatus of Obert et al. [17]. The three pairs of ball joints were employed to decrease the bending stress induced by the eccentricity
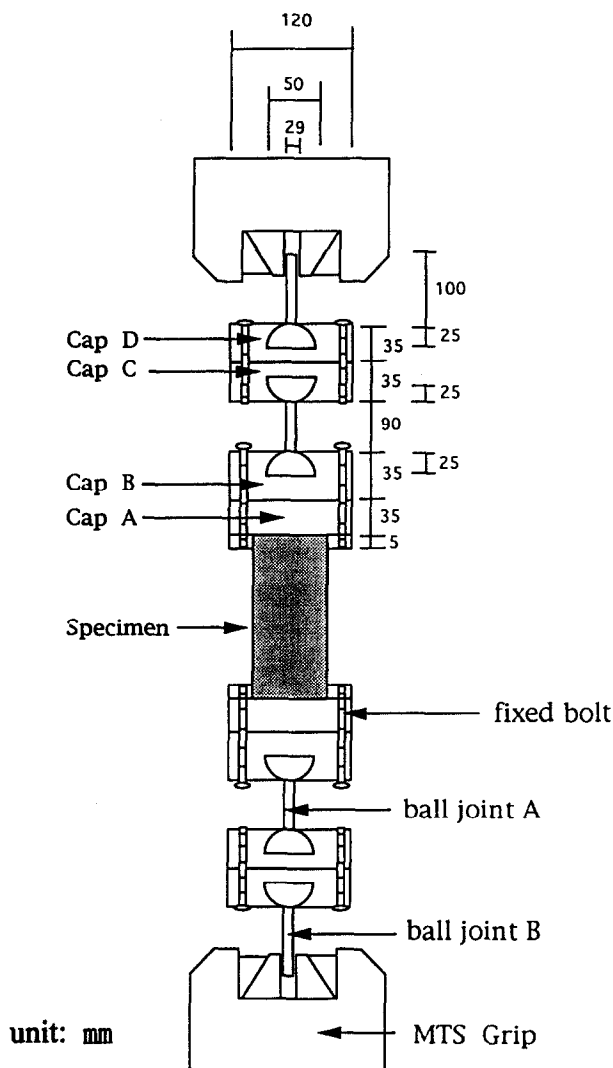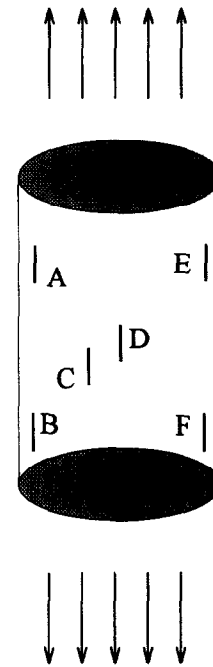

Fig. 2. Configuration of strain gages on the steel bar.

of the machine loading device. Then it can provide pure direct tensile loads on the testing specimen. Metal caps served to connect the ends of the rock specimen by epoxy resin. This method ensures that no friction forces are induced at the cylindrical surface of the specimen. To verify the quality of the tensile grip, a steel bar (UNS304) 54.7 mm in diameter and 136 mm in length was employed to conduct a direct tensile test by MTS 810 with a stress rate of 0.1 MPa per second. The steel bar is equipped with six strain gages at different locations on the surface (Fig. 2). The verification data are listed in Table 1. Experimental results indicate that the load is uniformly distributed on the steel bar. The calculated Young's modulus (189 Gpa) conforms closely to the given value (193 Gpa). The quality of this grip can confidently enable direct tensile tests to be performed on rock specimens.

Fig. 1. Assembly of the tensile grip.

Table 1. Verification data of the tensile grip

MPa	A	B	C	D	E	F
0.486971	2	3	2.5	2.5	3	3
0.995301	5	5.5	5	5	5	5
1.512174	8	8	7.5	8	8	8
2.020504	10.5	10.5	10	10.5	10.5	10.5
2.507475	13	13	13	13.5	13	13
3.015805	15	15.5	15.5	16	15.5	15.5
3.494233	17.5	18	18	18.5	18	18
3.998291	20.5	20.5	20.5	21.5	21	20.5
4.485263	23	23.5	23.5	24	23.5	23.5
5.019223	25.5	26	26	27	26	26
5.519009	28.5	28.5	29	29.5	28.5	28.5
6.00598	31	31	31.5	32.5	31.5	31
6.501495	33.5	34	34	35	34	33.5
7.02264	36.5	36.5	37	38	36.5	36.5
7.513883	39	39	40	40.5	39	39
8.017941	41.5	41.5	42.5	43	42	41.5
8.517727	44	44	45	46	44.5	44
9.000426	46.5	46.5	48	48.5	47.5	46.5
9.500213	49	49	50.5	51.5	49.5	49
9.991456	51.5	51.5	53.5	55	52.5	51.5

The unit of strain: 1×10^{-6}.

$\theta = 90°$

$0 < \theta < 90°$
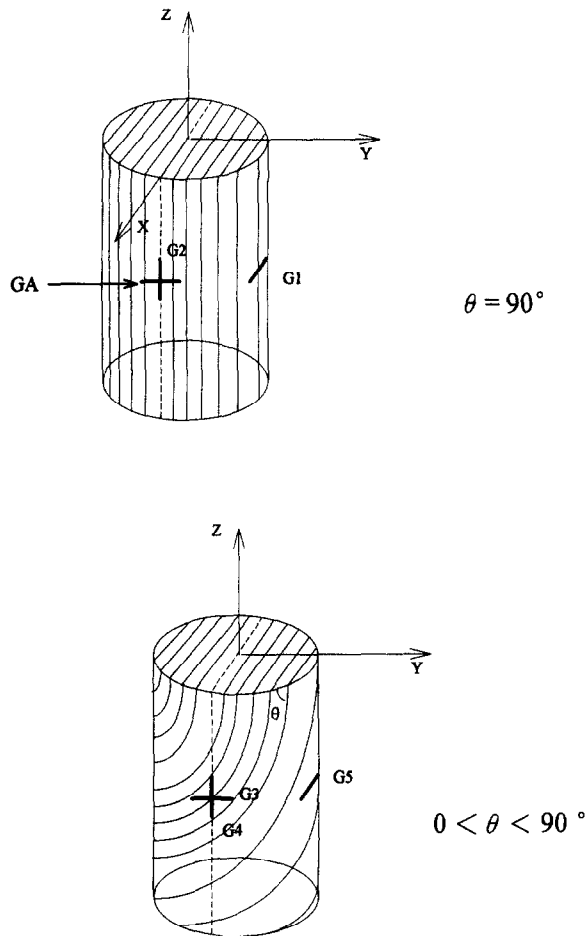
Fig. 3. Arrangement of strain gages on argillite specimens.

to the axial tension direction at stress rates of 0.1 MPa/sec. A stress rate of 0.01 MPa/sec was applied to conduct direct tensile tests of some specimens with low dipping angles for studying the stress–strain behavior of argillite. Positive tensile stress and positive extension strain are adopted in this article. The sign convention means that the negative lateral strain exhibits the contraction of the testing specimen at the location of a transversal gage.

Samples were prepared at the rock mechanics laboratory of National Chiao-Tung University (NCTU). Samples with NX size and L/D = 2.25–2.5 were cored with different inclinations of foliation planes with respect to the plane perpendicular to the tensile loading direction, starting from 0 to 90° with intervals of 15° from the block samples of argillite, i.e. θ = 0, 15, 30, 45, 60, 75, and 90°. For each inclination angle, five specimens were prepared for direct tensile tests. In order to verify the conceptual failure criterion proposed in this article, some extra specimens with θ of 80 and 85° were prepared. The block samples were collected from a construction site of a long highway tunnel (12.9 km in length with double 12.0 diameter tubes) in northern Taiwan. The core samples were prepared following the
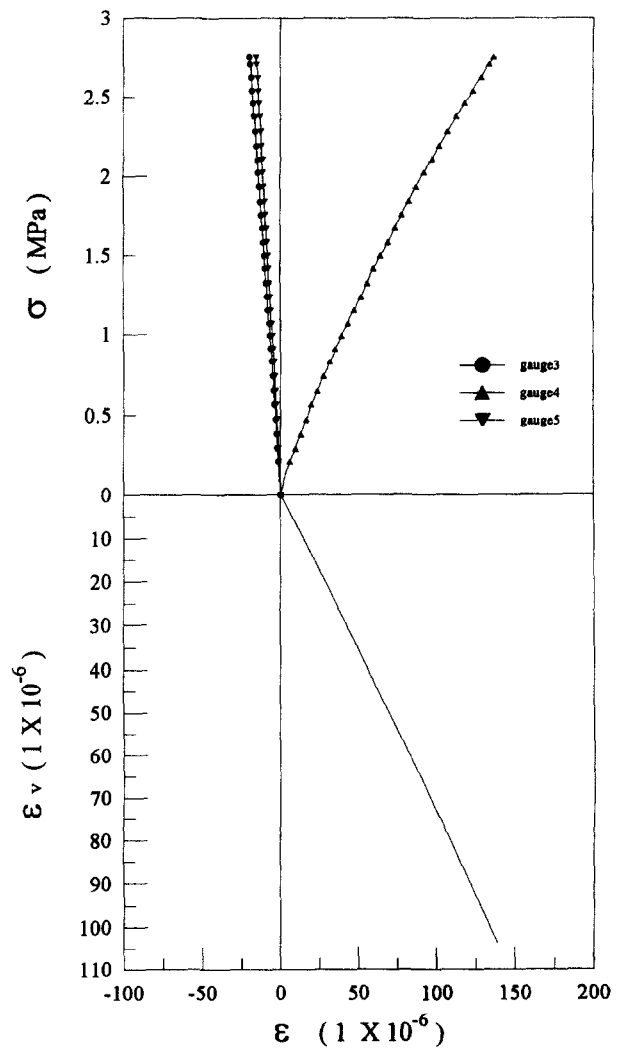
The cementing type of grip device was adopted in this study. Due to the difference between the physical properties of the metal caps and the rock specimens, the cementing material requires careful selection. The basic requirement for conducting a successful direct tensile test under a given loading rate is that the rock specimen breaks before the contact between the caps and the ends of the rock specimen fails. The tensile strength of the contacts must be greater than the maximum tensile strength of the rock specimen at the given loading rate. Various types of epoxy resin were tried for cementing the metal caps to the ends of rock specimens. Following the standard of ASTM D2950 (1993), only two epoxy resins, 3M 2216A/B and AA 600A/B, enabled the tensile strength of the contacts to be up to 15 MPa at a stress rate of 0.3 MPa/sec. Since strong anisotropy exists in the tensile strength of the argillite specimen, from a low 1.0 MPa up to 13 MPa, the data of load and strain for the specimens with low strength during testing at a 0.3 MPa/sec stress rate are not easily read because these specimens failed in a short time. In this study, we used a stress rate of 0.1 MPa/sec for the direct tensile test using stress control. However, for investigating the stress–strain behavior in direct tension, the data points of stress and strain are not enough for expressing the characteristics of the very low tensile strength argillite specimens, i.e. the specimens with a dipping angle of the foliation lower than 45° with respect to the plane normal

Fig. 4. The stress–strain relation of an argillite specimen with foliated planes of $\theta = 0°$.

Fig. 5. The stress–strain relation of an argillite specimen with foliated planes of $\theta = 15°$.

is small. A set of bridge boxes (model Kyowa DBB-120) and a set of strain amplifiers (model Kyowa DPM-611A/B) were connected to the strain gages and load cell for performing tests.

The argillite specimens were investigated in detail by microscopy. The composition of argillite is 45% quartz and 55% clay mineral (illite, chloride, . . .). The grain size of argillite is between that of silt and clay. Clear foliation planes are well-developed by the recrystallization of the clay mineral. The basic physical properties are: dry unit weight (26.3–2.72 KN/m³), specific gravity (2.71–2.75) and porosity (0.014–0.018). Argillite was formed from the slight metamorphism of shale or silty shale. Given a moderately increased degree of metamorphism, it will transform to slate. Argillite is commonly found in mountainous areas of Taiwan.

RELATION OF STRESS AND STRAIN

Based on the results of petrographic analysis, the argillite can be modeled as a transversely isotropic material due to the existence of clear foliation planes. Induced transverse strains in a small specimen of argillite vary from one location to another on the cylindrical
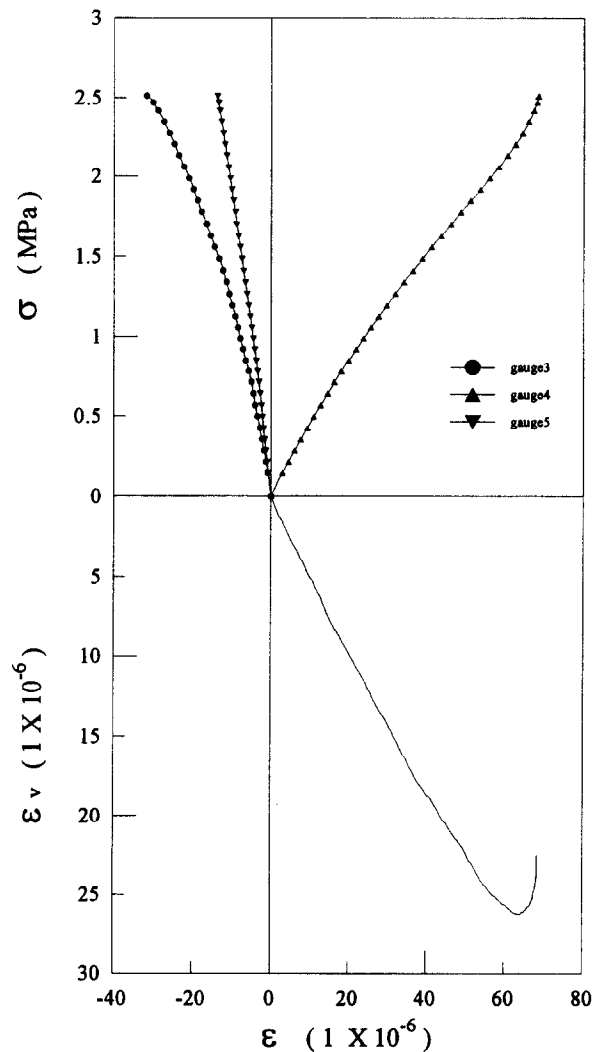
ISRM suggested method [20]. In order to investigate the stress–strain behavior, and calculate the elastic moduli in direct tension, one axial and two transverse strains were measured by attaching three sets of linear strain gages to the surface of the cylindrical specimen [21] (Fig. 3). The measured strains obtained from G1 to G5 in Fig. 3 were employed in order to calculate the five elastic moduli of transversely isotropic argillite. The average volumetric strain for the specimen with $\theta = 90°$ is the summation of the strains of G1, G2 and GA, and for the specimen with the $\theta \neq 90°$, the summation of the strains of G3, G4 and G5. The G2 and G4 strains were individually measured by a single piece of electrically resistant type of strain gage with a gage factor of two (model Kyowa KFG-5-120-c1-11). The induced transverse strain prior to failure of a brittle rock, such as the argillite specimen, under tension is very small, especially for specimens with low inclination angles. Hence, two strain gages (model Kyowa KFG-5-120-c1-11) with parallel arrangement or a semiconductor strain gage (model Kyowa KSP-2-120-F4) with a gage factor of 120, are attached to the positions of G1, G3, G5 and GA, for picking up a significant electric output and to obtain a transverse strain. The voltage output of the strain gage and load cell

Fig. 6. The stress–strain relation of an argillite specimen with foliated planes of $\theta = 30°$.
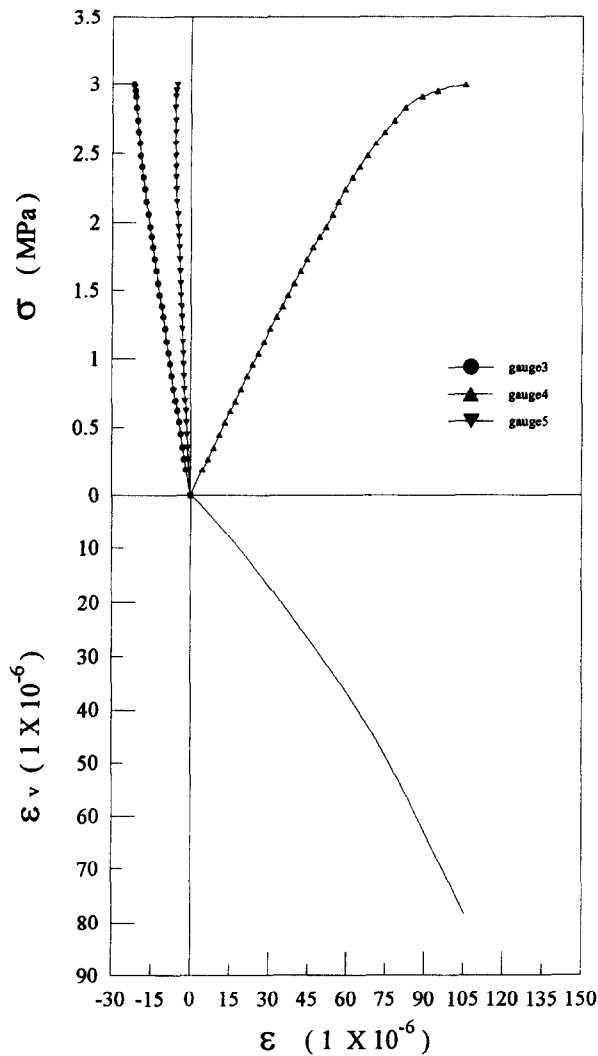
Fig. 7. The stress–strain relation of an argillite specimen with foliated planes of $\theta = 45°$.

indicate that (1) before specimens fail, the axial stress–axial strain curves exhibit a convex-upward trend for specimens with a high dipping inclination angle of foliation and (2) when the dipping angle of foliation is low, a concave upward trend is observed. These findings indicate that the micro-fissures which developed along the foliation planes cause the non-linear behavior of argillite under tension and reflect the fact that the degree of influence of the micro-fissures on tensile behavior is small when the angle θ is large. We conclude that the stress–strain behavior of transversely isotropic rocks strongly depends on the existence of micro-fissures in rocks with a dipping angle of less than 60° and that the influence of micro-fissures on the stress–strain behavior of rocks with a high dipping angle is slight.

Average volumetric strains during testing are also revealed in the figures for investigating the effect of the angle θ on the volume change under tension. The average volumetric strain (ε_v) is calculated as follows

$$\varepsilon_v = \varepsilon_1 + \varepsilon_2 + \varepsilon_A \tag{1}$$

for the specimens with $\theta = 90°$, and

$$\varepsilon_v = \varepsilon_3 + \varepsilon_4 + \varepsilon_5 \tag{2}$$

surface, except in the case of a specimen with $\theta = 0°$. Two transverse strains on the specimen surface with a 90° difference (Fig. 3) were measured for all the test specimens.

Figures 4–10 present the typical results of the observed stress–strain relations for the specimens with θ at 15° intervals from 0 to 90°. The relations of (1) uniaxial stress and uniaxial strain, (2) uniaxial stress and transverse strains, and (3) uniaxial strain and volumetric strain, are described in the figures. It is found that the strain reading at the corresponding location of different specimens with various values of θ is different for the same stress level. This means that the stress–strain behavior of argillite is anisotropic. The curve of axial stress vs axial strain is quasi-linear up to 50% ultimate tensile strength for specimens with an angle (θ) larger than 30°. For specimens with a low inclination of foliation, the curve exhibits apparent non-linearity before failure. Due to the closing of the pre-existing micro-fissures of a brittle fissured rock, a concave upward trend is clearly observed at the beginning of the stress–strain curve under compression [22]. However, no evidence of a concave-upward stress–strain section is observed in the figures for the direct tensile test. These
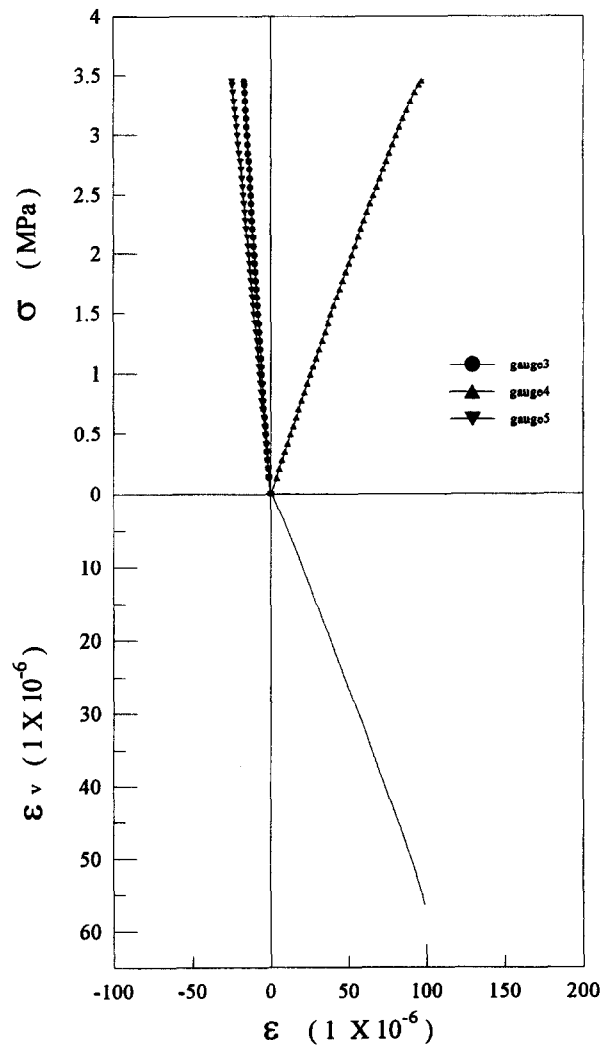

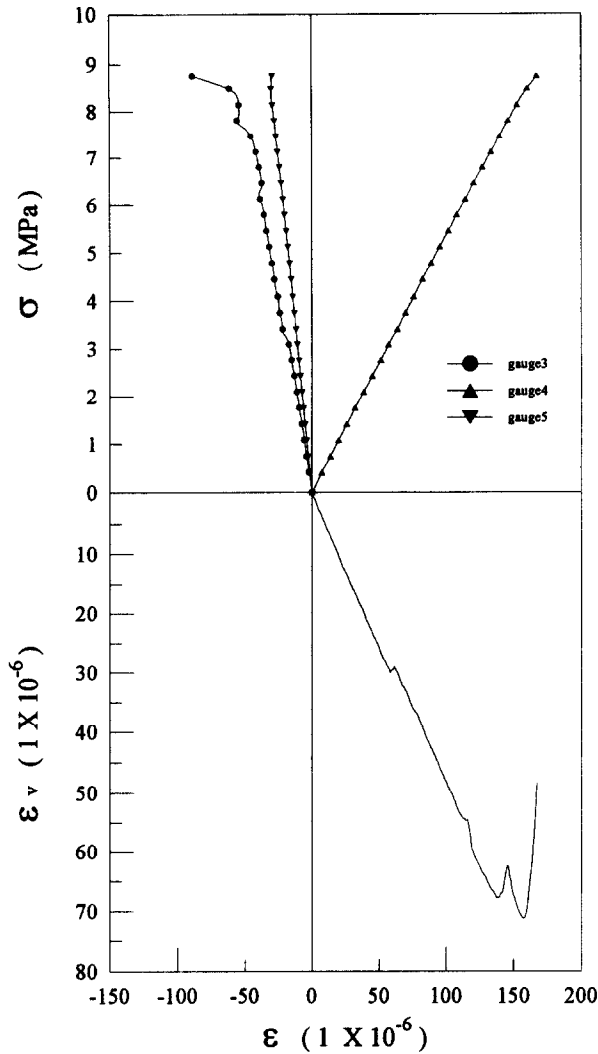Fig. 8. The stress–strain relation of an argillite specimen with foliated planes of $\theta = 60°$.

Fig. 9. The stress–strain relation of an argillite specimen with foliated planes of $\theta = 75°$.

for the specimens with $0° < \theta < 90°$, where ε_A, ε_1, . . ., and ε_5 are the measured strains of GA, G1, . . ., and G5 in Fig. 3, respectively. In fact, the sign of the transverse strain is different from that of the corresponding axial strain.

Figures 4–10 indicate that the average bulk volume at any stress level before failure is larger than that at test commencement for all specimens irrespective of the magnitude of the inclination angle of specimens. This indicates that the necking phenomenon before failure, like steel under tension, is not clear for this type of brittle rock. The average volume strain increases proportionally with an increase of axial strain and tensile loads as the axial stress–strain curve remains linear. Afterwards, the average volumetric strain decreases. This reflects the fact that the degree of the lateral strain increase is greater than the axial strain increase after the axial stress–strain curve becomes non-linear. This phenomenon is similar to that of a brittle rock in compression [22].

DEFORMABILITY OF ARGILLITE

As described above, argillite at some stress level can be modeled as a linear transversely isotropic elastic

material under tension. The generalized Hooke's law is adopted to express the material elastic behavior in an x', y', z' coordinate system. If the z' coordinate axis is normal to the planes of transverse isotropy, Hooke's law can be stated as follows:

$$
\begin{bmatrix} \varepsilon_{x'} \\ \varepsilon_{y'} \\ \varepsilon_{z'} \\ \gamma_{y'z'} \\ \gamma_{x'z'} \\ \gamma_{x'y'} \end{bmatrix} = \begin{bmatrix} \frac{1}{E} & -\frac{v}{E} & -\frac{v'}{E'} & 0 & 0 & 0 \\ -\frac{v}{E} & \frac{1}{E} & -\frac{v'}{E'} & 0 & 0 & 0 \\ -\frac{v'}{E'} & -\frac{v'}{E'} & \frac{1}{E'} & 0 & 0 & 0 \\ 0 & 0 & 0 & \frac{1}{G'} & 0 & 0 \\ 0 & 0 & 0 & 0 & \frac{1}{G'} & 0 \\ 0 & 0 & 0 & 0 & 0 & \frac{1}{G} \end{bmatrix} \begin{bmatrix} \sigma_{x'} \\ \sigma_{y'} \\ \sigma_{z'} \\ \tau_{y'z'} \\ \tau_{x'z'} \\ \tau_{x'y'} \end{bmatrix} \quad (3)
$$

where E and E' are Young's moduli in the plane of transverse isotropy, and in a direction normal to it, respectively. v and v' are Poisson's ratios characterizing the lateral strain response in the plane of transverse isotropy to a stress acting parallel, or normal to it,
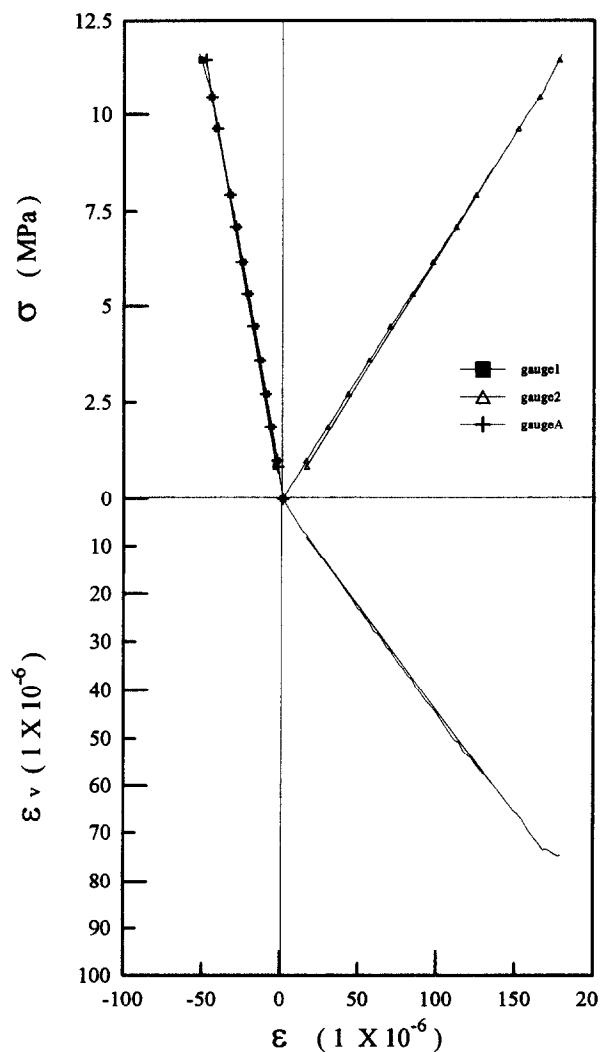

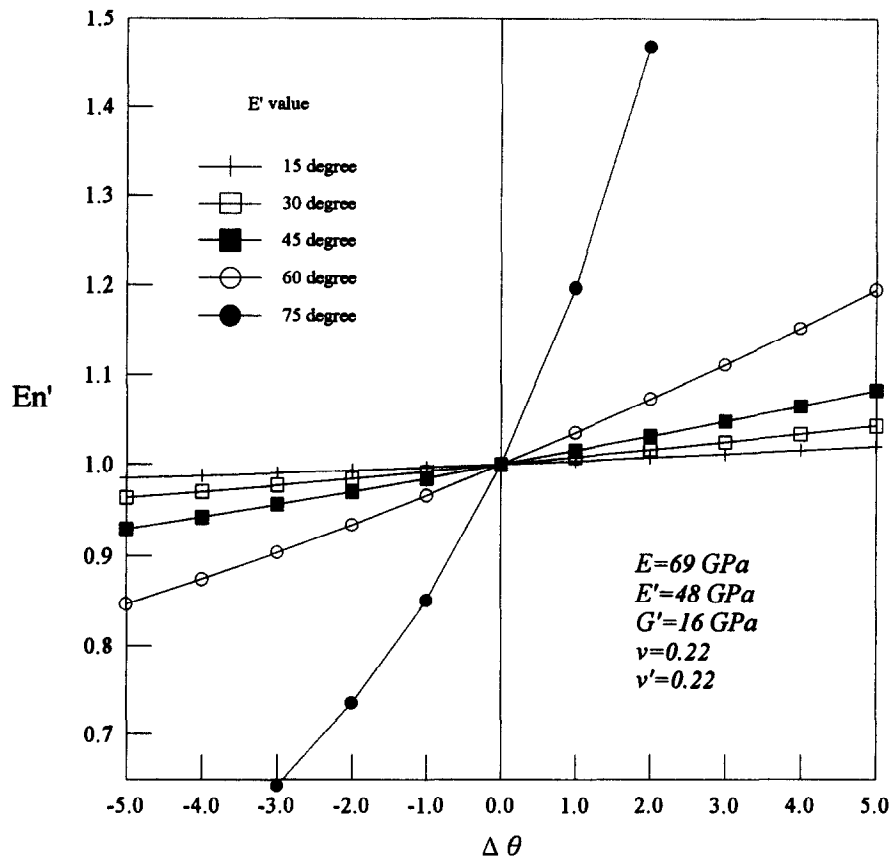Fig. 10. The stress–strain relation of argillite specimen with foliated planes of $\theta = 90°$.

Fig. 11. Variation of the normalized elastic constant E'_n with a possible dipping angle error.

respectively and, G' is the shear modulus in planes normal to the plane of transverse isotropy.

The five elastic constants of a transversely isotropic rock can be determined from a series of tests in the laboratory, or in the field by static or dynamic tests. Only a static test in a laboratory is of relevance in this study. The accuracy of the results of testing the deformability of rocks depends on the homogeneity of the testing sample and the reliability of the measured data, among others. Unlike isotropic rocks, the five elastic moduli of transversely isotropic rocks cannot be calculated from the test data of a single specimen. Previous studies suggested that two or three specimens be used with differently inclined angles of elastic symmetric planes with respect to the major loading direction for performing compressive tests to obtain the five elastic moduli [8, 10, 21]. Two cylindrical specimens, with attached strain gages on the specimen surface (Fig. 3), served for performing a loading test to calculate the five elastic moduli of argillite under tension. Based on the generalized Hooke's law and the choice of a coordinate system related to the planes of elastic symmetry, the five elastic constants of a specimen of transversely isotropic rock, with loading tests according to the configuration as depicted in Fig. 3, are given as follows [21]:

$$E = \frac{1}{M_2}, \quad v = -\frac{M_1}{M_2} \qquad (4)$$

$$\frac{1}{G'} = M_4 \csc^2 \beta - M_3 \sec^2 \beta$$
$$+ (0.5 \cos^2 \beta/G + M_5)(\sec^2 \beta - \csc^2 \beta) \qquad (5)$$

$$\frac{1}{E'} = (M_3 + M_4 - \cos^2 \beta/E) \csc^2 \beta$$
$$- M_5 \csc^4 \beta - \cot^2 \beta \csc^2 \beta v/E \qquad (6)$$

$$\frac{v'}{E'} = -(M_5 + \cos^2 \beta v/E) \csc^2 \beta, \qquad (7)$$

where β is the angle between the tensile loading direction and the foliation planes of specimen, $\beta = \pi/2 - \theta$. $M_1 = \varepsilon_{g1}/\sigma_1$, $M_2 = \varepsilon_{g2}/\sigma_1$, $M_3 = \varepsilon_{g3}/\sigma_3$, $M_4 = \varepsilon_{g4}/\sigma_3$, $M_5 = \varepsilon_{g5}/\sigma_3$. Both the elastic moduli E and v are obtained from the measured data of a specimen with foliation planes parallel to the tensile direction ($\beta = 0°$). However, the other three elastic moduli E', v' and G' are to be calculated from the measured data of a specimen with an inclined angle (β) of foliation corresponding to the loading direction, and the induced results of E and v obtained from the specimen with $\beta = 0°$. Due to the unclearness of the foliation planes on the cylindrical surface of the argillite specimens, it is not easy to judge the foliation plane dipping angle accurately by eye. There is a possible error of 5° in the measurement of this angle in the prepared specimens employed in this research. However, the calculated deformability of transversely isotropic rocks is dependent on the inclination of planes of transverse isotropy. The influence of the inclination on the calculated elastic moduli, E', v' and G', from equations (5)–(7) requires further investigation. One set of known elastic moduli, five dipping angles ($\theta = 15$, 30, 45, 60 and 75°) and a given stress served as input data for solving the
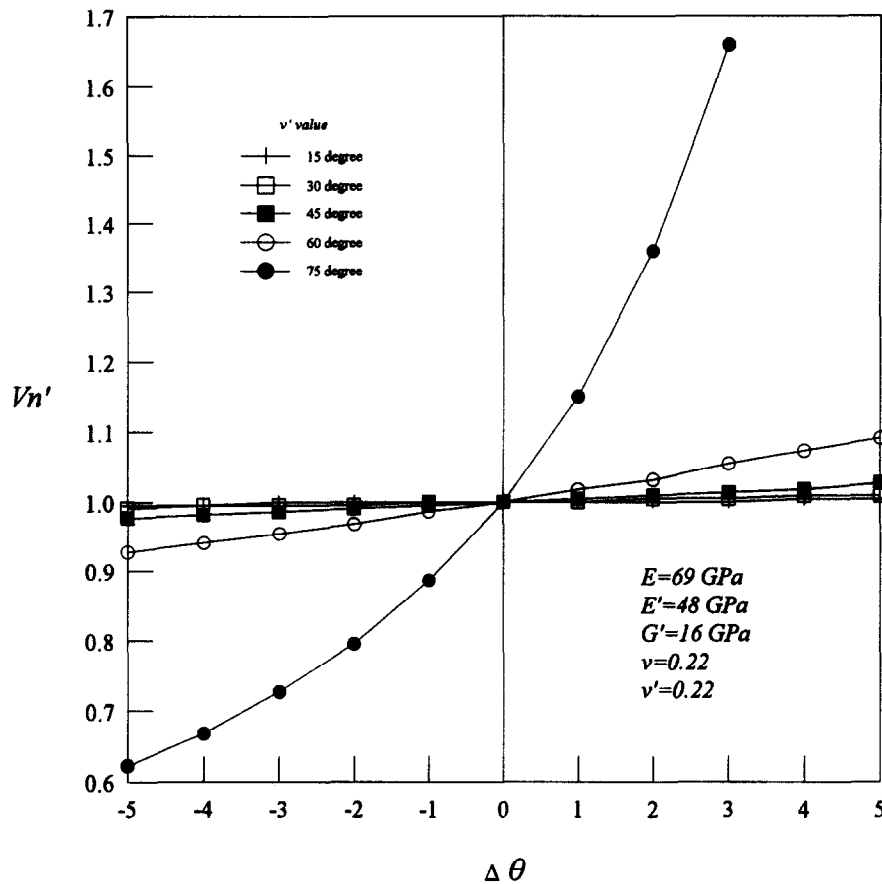
Fig. 12. Variation of the normalized elastic constant v'_n with a possible dipping angle error.

generalized Hooke's law [equation (3)] in order to obtain the idealized induced strains compared to the readings of the three strain gages in Fig. 3. Then, the idealized induced strains served as the input data for equations (5)–(7) to calculate the apparent theoretical elastic moduli, E', v' and G', at 1° intervals from −5 to 5° difference from the given dipping angle (e.g. 10, 11, . . ., 19, 20°, which are the possible dipping angles judged by the eye, for the given angle 15°). The normalized apparent elastic moduli (E'_n and v'_n), normalized by the corresponding true elastic moduli (e.g. the elastic moduli of 11° divided by that of 15°), vary with the possible dipping angles, as is depicted in Figs 11 and 12. The results show that the elastic moduli obtained from a specimen with a high inclination of foliation are sensitive to varying the selection of the input inclination angle. The variation of the elastic moduli with the input θ is small for specimens with a low θ. However, for the specimen with a very low θ, the elastic modulus G' becomes impossible to deduce because no significant difference between the two measured transverse strains

can be adopted as an input for equation (7). We recommend that to obtain the three elastic moduli, an inclination angle of foliation between 30 and 60° of the test specimen is preferable.

The argillite specimens in our tests served for performing direct tensile tests. The applied loads and induced strains were recorded. The relevant data for loads and strains obtained from specimens with dipping angles of 90, 45 and 30° are utilized to calculate the five elastic moduli by equations (4)–(7). The average calculated results of the tangential moduli at 25% uniaxial tensile strength are listed in Table 2. They indicate that the argillite models well as a transversely isotropic material. Liu *et al.* [23] investigated the deformability of argillite under uniaxial compression by the method suggested by Wei and Hudson. They presented the results of the five elastic moduli as shown in Table 2. Compared with the test results of argillite specimens under uniaxial compression, the magnitude of elastic moduli E, v,v' and G' in uniaxial tension closely follows that of uniaxial compression. However, the value

Table 2. Elastic constants of argillite specimens in tension and in compression

Specimen, dip angle (θ)	Elastic const.	E (GPa)	v	E' (GPa)	G' (GPa)	v'	Test compression
30				51.14	15.61	0.22	Direct
45		59.09	0.22	51.86	14.91	0.1	tension
20				37.28	12.36	0.16	*Uniaxial
45		51.82	0.19	32.24	13.26	0.18	compression

*From ref. [23].
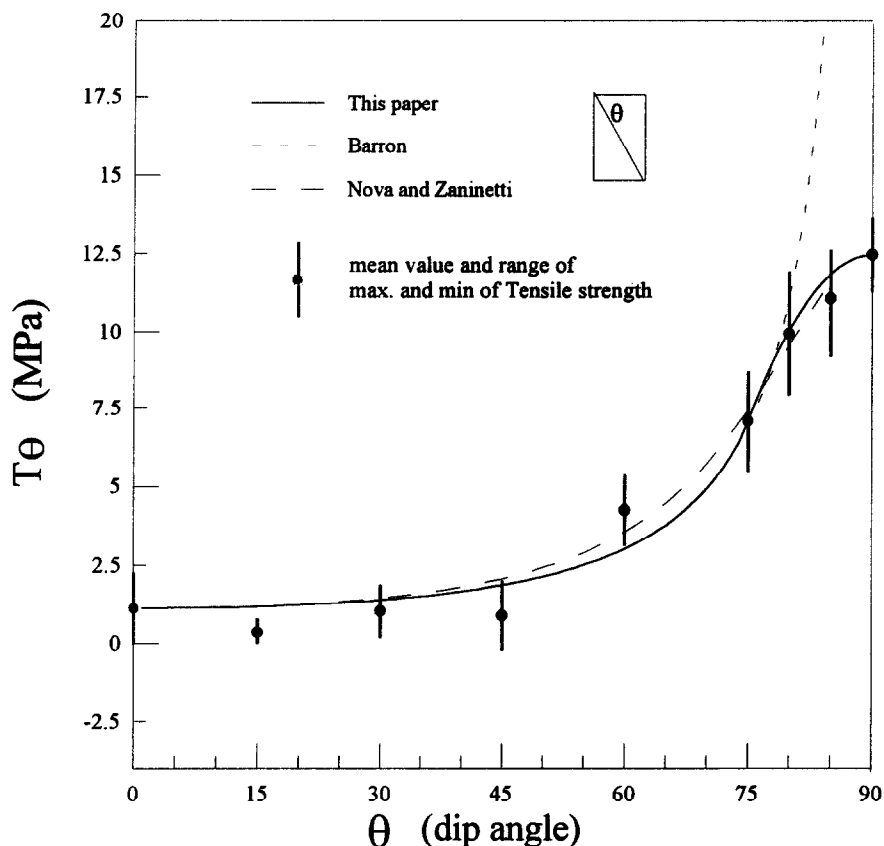
Fig. 13. Tensile strength of argillite specimens and its failure criteria.

TENSILE STRENGTH OF ARGILLITE

The test results of the direct tensile strength of the argillite specimens with different orientations are listed in Fig. 13. The tensile strength is defined as the ultimate load divided by the original cross-sectional area of the test specimen. It is found that the trend of the direct tensile strength with respect to the foliation planes is clear, i.e. the tensile strength increases with the increase of dipping angle. Due to specimen non-homogeneity, much scatter exists in the measured data of different specimens with the same inclination. Following the testing and investigating in detail, the final failure modes of the test specimens were observed. Figure 14 displays the photographs of typical failed specimens. It is clear that specimens with dipping angles of 0, 15, 30, 45 and 60° fail along the foliation. This indicates that the failure of argillite specimens is induced from the tip propagation of the pre-existing micro-fissures along the foliation.

of the elastic modulus E' under uniaxial tension is greater than that under compression. These results reflect the fact that the degree of influence of pre-existing micro-fractures in the test specimen on E' is greater than on that of the others due to the major pre-existing micro-fissures developed in parallel with the foliation planes. It also indicates that the elastic constants obtained from the uniaxial tensile test are more conservative than those obtained from the compression test with regard to rocks being modeled as a linear elastic material.

However, for a specimen with a 75° inclination angle, failures partly along and partly through the foliation were observed. The failure plane exhibits a sawtoothed shape. For specimens with the foliation parallel to the tensile direction, the failure plane also exhibits a clear sawtoothed shape, but only a few parts of the failure plane occur along the foliation. The phenomenon of the sawtoothed failure plane reflects the fact that the progressive failure occurs during direct tensile tests. The progressive failure may include primary tensile cracks (developed perpendicular to the tensile loading direction) and secondary cracks, parallel to the foliation (induced by the tip propagation of the primary tensile cracks). The evidence of the sawtoothed failure mode has neither been mentioned nor adopted to develop a tensile failure criterion in the literature [13, 16]. As described above, the existing criteria are not satisfactory for dealing with the failure mechanism in direct tension when the foliation of specimens is parallel or inclined at a small angle to the uniaxial tensile loading direction.

Based on the failure phenomena of the tested argillite specimens, a failure criterion of direct tensile strength is proposed for anisotropic rocks as follows:

$$T_\theta = \frac{4T_0}{(1 + \cos(2\theta)) + \sqrt{2(1 + \cos(2\theta))}} \qquad (8)$$

or

$$T_\theta = T_{90}(1 - c\cos^2(\theta)) \qquad (9)$$

where T_0 and T_{90} are the direct tensile strengths of the rock specimens with the inclination angle (θ) 0° and 90°,

respectively, of foliation, and c is a material constant which depends on the rock types and its fracture modes.

For the specimens in which the failure plane coincides with the foliation planes, the tensile failure criterion developed by Barron [13] [equation (8)] on the basis of the Griffith theory, is directly adopted in this paper. However, a conceptual model is given [equation (9)] to fit the specimens with a high dipping angle of the foliation. This model is based on the above described failure factors (Fig. 15), where the idealized specimen with a sawtoothed failure indicates that the specimen fails partly along and partly through the foliation. The symbol "I" in Fig. 15 depicts the part of the failure occurring along one of the n foliated planes. Compared with the tensile strength of the part of the failure through the foliation, the strength along foliation can be neglected. The value of c in equation (9) depends on the rock types and the failure mode. The value of c can be estimated from the test data of specimens that have failed with a sawtoothed plane by regression. In this paper, equation (9) is employed to predict the tensile strength of argillite specimens with $\theta = 75°$–$\theta = 90°$. The c value of argillite specimens is equal to 6.5 for the proposed criterion. Figure 13 gives the predicted tensile strength of equation (9) and the existing models. In Fig. 13, the data of predicted line for the Barron's

model are calculated from equation (8); the failure cure for the criterion proposed by Nova and Zaninetti [16] is plotted by:

$$T_\theta = \frac{T_M T_m}{T_m \sin^2(\theta) + T_M \cos^2(\theta)} \tag{10}$$

in which T_M and T_m are the maximum and minimum tensile strengths, respectively.

Since the failure modes have been adopted in the proposed criterion, the predicted curve of equation (9) correlates closely with the experimental data for argillite specimens.

CONCLUSIONS

A tensile grip employed with a servocontrolled material testing machine, was developed for performing high quality, direct tensile tests. This tensile grip comprises a steel rod with three pairs of ball joints. The very small transverse strain on the specimens was measured by means of a semiconductor strain gage or two pieces of electrically resistant type of strain gage with a parallel arrangement. The tensile behavior of argillite is modeled as a transversely isotropic rock.

$\theta = 0^0$ $\theta = 15^0$ $\theta = 30^0$ $\theta = 45^0$

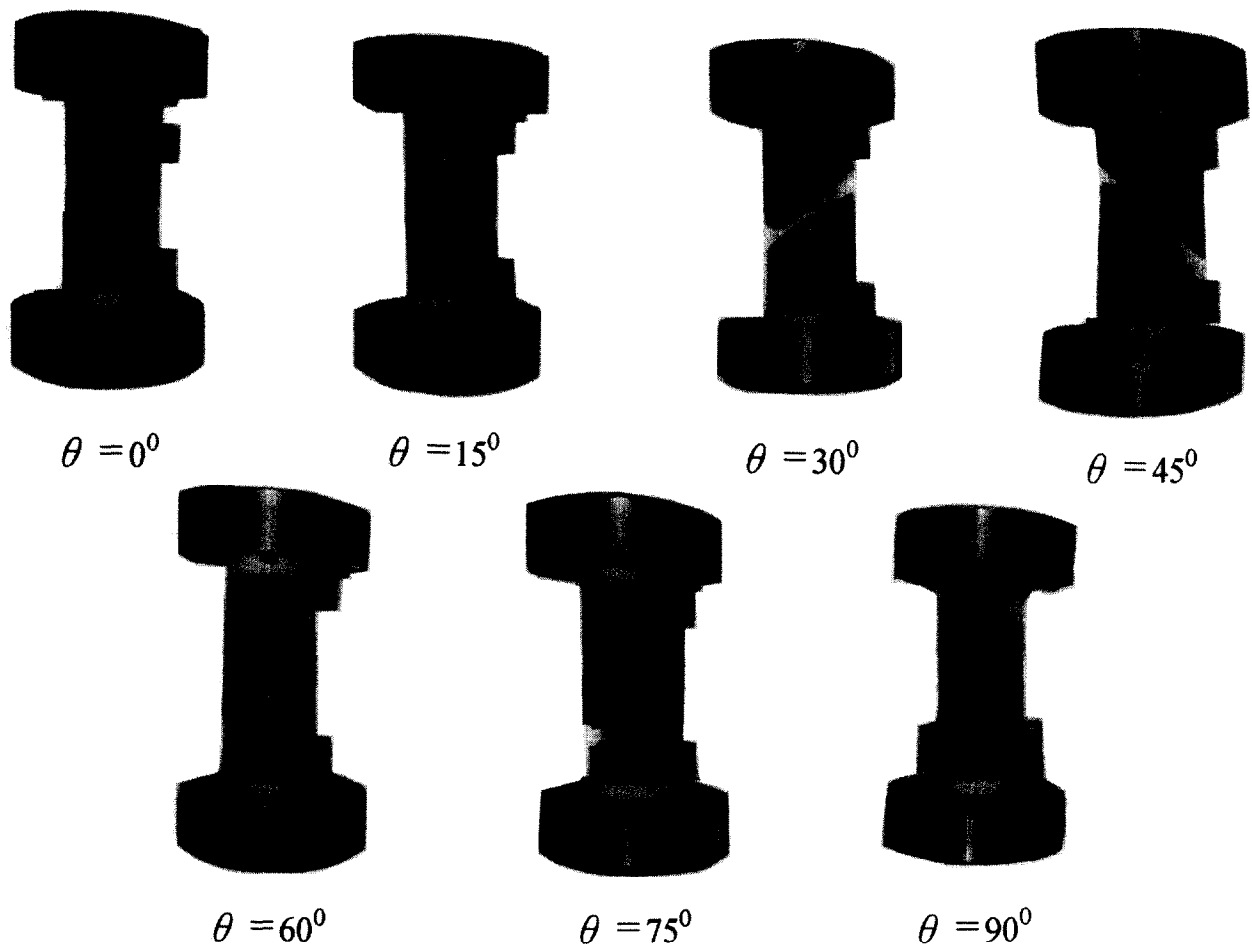$\theta = 60^0$ $\theta = 75^0$ $\theta = 90^0$
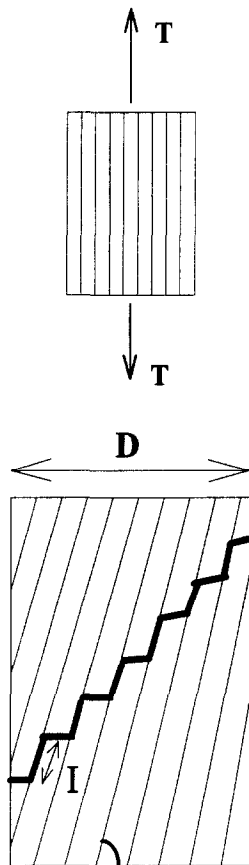
Fig. 14. Typical failed specimens.

Fig. 15. Conceptual failure mode of specimens with a high inclination of foliations.

Based on the experimental results and a theoretical analysis, the following conclusions are given:

(1) The stress–strain behavior of argillite under tension is anisotropic. It strongly depends on the existence of micro-fissures that have developed along foliation. For specimens with a high inclination of foliation ($\theta \geq 45°$), the stress–strain curve is quasi-linear and exhibits a convex-upward before specimen failure. On the other hand, the curve for specimens with a θ lower than 45° is apparently non-linear and exhibits a concave-upward trend before specimen failure. The average bulk volume for all test specimens at any stress level before failure is greater than that at test commencement irrespective of the magnitude of the inclination angle of foliation of specimens. The average volume strain increases proportionally with an increase in axial srain and in tensile loads up to the deviation of the linear part of the axial stress–axial strain curve.

(2) The five elastic constants of a transversely isotropic rock are readily calculable by measuring two cylindrical specimens ($\theta = 90°$ and $0° < \theta < 90°$), as suggested by Wei and Hudson [21]. Taking into account specimen non-homogeneity and the unavoidable element of experiment error, a specimen with a $\theta = 30–60°$ is recommended as a feasible choice for obtaining the elastic moduli (E', G' and v') under compression or tension.

(3) The magnitude of the elastic constants, E, G', v and v', calculated from the direct tensile test, corresponds closely to that obtained from the uniaxial compression test. Without the micro-fissures closing during tension, the magnitude of E' under tension exceeds that of under compression. For rocks being modeled as a linear elastic material, the elastic moduli of transversely isotropic rock obtained from an uniaxial tensile test are more conservative than those obtained from a compression test.

(4) Two types of failure plane are observed: a sawtoothed type for specimens with a θ closer to the 90° plane perpendicular to the loading direction and a smooth type along foliation for specimens with a low θ. The sawtoothed failure plane reflects the fact that the progressive failure occurs during direct tensile testing. Because the failure mode is adopted, the proposed tensile failure criterion matches closely with the experimental data of argillite specimens.

REFERENCES

1. Goodman R. E. *Introduction to Rock Mechanics*, 2nd edn. John Wiley, Singapore, 1989, pp. 55–57.
2. Lekhnitskii S. G. *Theory of Elasticity of an Anisotropic Body*. Mir Publisher, Moscow, 1979, p. 37.
3. Liao J. J. and Amadei B. Surface loading of anisotropic rock masses. *J. Geotech. Engng, Am. Soc. Civ. Engrs*, 1991, **117**, 1779–1800.
4. Jaeger J. C. Shear failure of anisotropic rocks. *Geol. Mag.*, 1960, **97**, 65–72.
5. McLamore R. and Gray K. E. The mechanical behavior of anisotropic sedimentary rocks. *J. Engng Industry, Trans. Am. Soc. Mech. Engrs Ser. B*, 1967, **89**, 62–73.
6. Donath F. A. Effects of cohesion and granularity on deformational behavior of anisotropic rock. In *Studies in Mineralogy and Precambrian Geology*, Vol. 135 (Edited by Doe B. R. and Smith D. K.). Geol. Soc. Am. Memoir, 1972 **135**, pp. 95–128.
7. Nova R. The failure of transversely isotropic rocks in triaxial compression. *Int. J. Rock Mech. Min. Sci. & Geomech. Abstr.*, 1980, **17**, 325–332.
8. Homand F. and Morel E. Characterization of the moduli of elasticity of an anisotropic rock using dynamic and static methods. *Int. J. Rock Mech. Min. Sci. & Geomech. Abstr.*, 1993, **30**, 527–535.
9. Kwasniewski M. A. Mechanical behavior of anisotropic rocks. In *Comprehensive Rock Engineering—Principles, Practice & Projects*, Vol. 1 (Edited by Hudson J. A. and Brown E. T.). Pergamon Press, Oxford, 1993, pp. 285–312.
10. Ramamurthy T. Strength and modulus responses of anisotropic rocks. In *Comprehensive Rock Engineering—Principles, Practice & Projects*, Vol. 1 (Edited by Hudson J. A. and Brown E. T.). Pergamon Press, Oxford, 1993, pp. 313–325.
11. Hobbs D. W. The tensile strength of rocks. *Int. J. Rock Mech. Min. Sci. & Geomech. Abstr.*, 1964, **1**, 385–396.
12. Hobbs D. W. Rock tensile strength and its relationship to a number of alternative measures of rock strength. *Int. J. Rock. Mech. Min. Sci. & Geomech. Abstr.*, 1967, **4**, 115–127.

13. Barron K. Brittle fracture initiation and ultimate failure of rocks—Part 1: isotropic rocks; Part 2: anisotropic rocks—theory; Part 3: anisotropic rocks—experimental results. *Int. J. Rock Mech. Min. Sci. & Geomech. Abstr.*, 1971, **8**, 541–575.

14. Barla G. and Innaurato N. Indirect tensile testing of anisotropic rocks. *Rock Mech.*, 1973, **5**, 215–230.

15. Barla G. and Goffi L. Direct tensile testing of anisotropic rocks. *Proc. 3rd Int. Congr. Rock Mechanics*, Vol. 2, Part A, Denver, 1974, pp. 93–98.

16. Nova R. and Zaninetti A. An investigation into the tensile behavior of a schistose rock. *Int. J. Rock Mech. Min. Sci. & Geomech. Abstr.*, 1990, **27**, 231–242.

17. Obert L., Windes S. L. and Duvall W. I. Standardized tests for determining the physical properties of mine rocks. *U.S.B.M.R.I.*, *1946*, **3891**.

18. Hawkes I. and Mellor M. Uniaxial testing in rock mechanics laboratories. *Engng Geol.*, 1970, **4**, 177–185.

19. ASTM, Standard test method for direct tensile strength of intact rock core specimens, 1993, D 2936–84.

20. International Society for Rock Mechanics Commission on Standardization of Laboratory and Field Tests. Suggested methods for determining tensile strength of rock materials. *Int. J. Rock Mech. Min. Sci. & Geomech. Abstr.*, 1978, **15**, 99–103.

21. Wei Z. Q. and Hudson J. A. Testing of anisotropic rock masses. *Proc. Confer. Appli. Rock Engng*, The University of Newcastle upon Tyne, U.K., 1988, pp. 251–262.

22. Goodman R. E. *Introduction to Rock Mechanics*, 2nd edn. John Wiley, 1989, p. 70.

23. Liu J.-Y., Liao J. J. and Wang C. D. Deformability of transversely isotropic rocks. *Proc. 94 Rock Engng Symp. Taiwan.* The National Central University, Chungli, Taiwan, 1994, pp. 101–110 (in Chinese).